Influence of machine-side filaments and jet-to-wire speed ratio on the flow through of a forming fabric

ALI VAKIL, ARASH OLYAEI, AND SHELDON I.GREEN

ABSTRACT: In the forming section of a paper machine, pulp is spread over a moving fabric and water is drained through the fabric. The fibers left behind form a wet sheet. The mechanical dewatering that begins in the forming section is important to the final paper quality because any non-uniformities arising in this section cannot be corrected later in the paper machine. Therefore, understanding the flow field through the forming section provides insight into the finished paper.

We analyzed the effect of the machine-side filaments of the fabric on the flow field upstream of the paper-side filaments. The resistance of a multilayer fabric was found to be nearly equal to the sum of the resistances of each layer considered in isolation. For the particular fabric, the machine-side layer produced up to a 10% effect on the velocity above the paper-side layer. For the effect of jet-to-wire speed ratio on the flow, an angled approach flow to the fabric produced very little change in the average flow perpendicular to the fabric (i.e., little change in fabric permeability). However, it has a marked effect on the machine-direction shear stress in the vicinity of the paper-side filaments. This shear stress drives the fiber orientation characteristics of so-called rush or drag jet impingement.

Application: Fabric manufacturers will gain new insight into flow-through forming fabrics, which may suggest some fabric design improvements. Fabric suppliers to mills will gain insight into the tradeoff between selecting fabrics for long life and superior drainage/retention characteristics.

In a companion article [1], we described a novel method to accurately model forming fabrics. Based on an analytical technique, we predicted the particle distribution in the flow fields. The flow nonuniformity and its probable effect on particles were dealt with both on the scale of filaments and a larger-scale, weaved-based non-uniformity. In this paper, we continue the studies on forming fabrics.

In the papermaking process, a dilute suspension of pulp fibers is spread over a forming fabric to mechanically drain water from the suspension [2]. Good forming fabrics are characterized by low running resistance, good fibers retention, and longer life. A single-layer fabric can enhance the water removal from the suspension, but at the cost of decreased retention. In contrast, a multilayer fabric exhibits superior fiber retention and life, but an inferior drainage rate [3, 4].

The mass distribution of the fibers in the sheet, i.e., the formation or macroscale nonuniformity, is affected by the fabric weave structure and number of layers [5]. The systematic variation in the distribution and orientation of the fibers, fines, and fillers in finished paper is known as wire mark [6]. It is postulated that the flow nonuniformity produced by the structure of a fabric can unevenly distribute the pulp fibers, producing a hydrodynamic wire mark. The wire mark can be distinguished from random variation by examining the frequency spectrum of the printed structure [6, 7].

The flow nonuniformity may occur on three different scales: (1) the filament diameter, (2) the weave pattern, and (3) the edge flow. We are concerned here with nonuniformity on the scale of the filament and the weave pattern, as this nonuniformity can have a profound effect on the quality of the printed end product [8, 9].

The fiber orientation distribution in a sheet arises from two sources: (1) the fiber orientation in the headbox and (2) fiber redistribution that occurs on and after jet impingement on the fabrics. Fiber orientation before and upon impingement is known to have a tremendous effect on the final paper properties [10, 11]. Strength, smoothness, tensile, and tear ratio properties are tightly connected with fabric characteristics such as air permeability, drainage capacity, and fiber support [12].

At high Reynolds numbers, the pressure drop through fabrics correlates with the dynamic pressure, ρV^2, where V is the bulk flow velocity and ρ is the fluid density. In contrast, at low Reynolds numbers, the pressure drop correlates with $\mu V/L$ (Darcy's Law), where μ is the fluid viscosity and L is a characteristic length scale. At intermediate values of Reynolds number, it is common to approximate the pressure drop as the sum of Darcy's Law and dynamic pressure terms, $\Delta P = a\mu V + b\rho V^2$. There are some published works presenting pressure drop-flow rate relationships and relating the coefficients a and b to the fabric geometrical properties [13–17].

The complexity of the flow and fiber/fabric interaction has limited much previous work to the pure water through two-dimensional (2D) model forming fabrics. In those investigations, the forming fabrics were modeled as banks of nonuniform cylinders [18, 19]. It was found that if the surface spacing between the two rows was greater than 0.7 d (d being the paper-side filament diameter), then the upstream flow field remained fairly unaffected by the presence of the second layer. Three-dimensional (3D) simulations of flow through single-layer fabrics have also been done [20] on the effect of lateral displacement of filaments on the nonuniformity of the flow through the adjacent unperturbed apertures.

Old single-layer forming fabrics were supplanted by a new generation of multilayer fabrics to meet two major requirements: (1) increasing mechanical stability and lifespan on the machine-side layer using larger cross-direction yarns and (2) improving formation on the top layer by using finer yarn [5]. Although a multilayer fabric improves fiber retention and reduces the flow nonuniformities, it generally leads to lower drainage rates. It has been postulated that machine-side fabric filaments may adversely affect the flow field on the paper-side filaments. As one part of the present study we investigate this effect. We simulated the flow through a real industrial fabric and also its machine-side and paper-side layers separately, and inferred from the flow field differences the effect of machine-side on paper-side flow. We also modeled the jet-to-wire speed ratio by inclining the inlet volume of simulations and compared the spatial distribution of velocity between normal and inclined incoming flow to the fabric.

NUMERICAL METHOD

Meshing and boundary conditions

In comprehensive modeling of the flow field through forming fabrics, the fibers suspended in the water and the free surface interaction between the suspension phase and the surrounding air must be taken into account. In this article, we do not discuss the water-air interface or fibers in the suspension; therefore, we simulate a pure water flow through forming fabrics, which owing to the low Reynolds number is laminar. **Figure 1** shows these phases and a schematic of jet impingement on the fabric.

The first stage of dewatering is conceptualized as follows: (1) free-jet zone in which the suspension jet travels between the headbox and the location where it impinges on the fabric, (2) oblique-dewatering zone where the jet has just impinged on the fabric, and (3) perpendicular-dewatering zone where the suspension drains in the Z-direction. In our previous article [1] we directed our attention only to the third region so the computational domain was constructed to simulate a flow normal to the fabric. In this paper, we compared spatial differences in velocities and shear stresses between perpendicular and oblique dewatering.

In papermaking, the incoming jet impinges on the fabric with angles in the range $3° < \alpha < 10°$, as observed in the frame of reference of the paper machine. In terms of the fabric reference frame, this impingement angle, θ, is (Eq. 1):

$$\tan\theta = \frac{R_{JW} \times \sin\alpha}{R_{JW} \times \cos\alpha - 1} \quad (1)$$

where $R_{JW} = V_J/V_W$ is the jet-to-wire speed ratio, which is normally between 0.990 and 1.035 [21]. Therefore, for an impingement angle of $\alpha = 5°$ with an $R_{JW} = 1.035$, the corresponding angle in the fabric reference frame would be $\theta \approx 70°$.

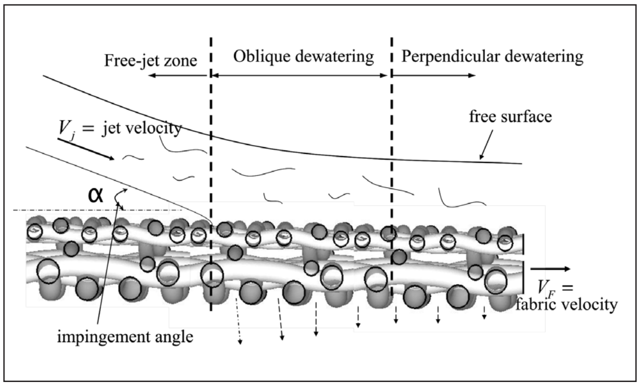

1. Schematic of fabric and impinging jet.

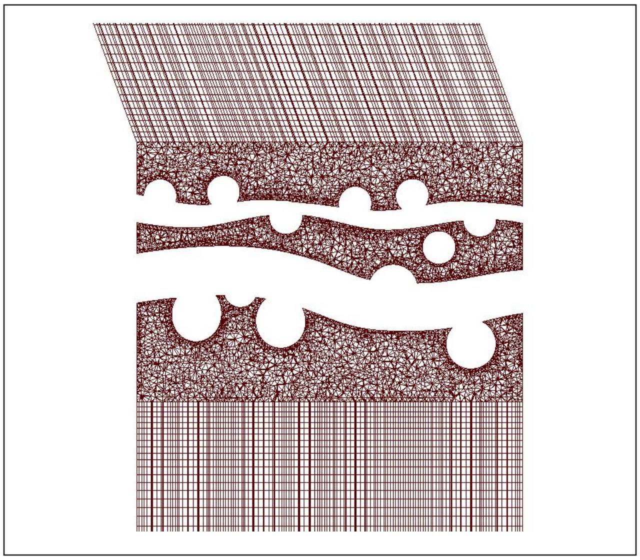

2. Hybrid computational mesh scheme.

The 3D modeling of fabrics based on 2D X-ray microtomography was described thoroughly in [1]. In brief, a MATLAB code identifies circular and elliptical cross sections, either isolated or blended, among the objects in each image. The resulting data are smoothed by generating a 3D spline through them. Filament volumes are then constructed by sweeping ellipses along each fitted spline.

When a 3D model of the fabrics is built, a yarn volume is created around it that contains tetrahedral elements around the fabric. The yarn volume is then extended downstream to create the outlet volume, and upstream of the yarn volume is an inlet volume. For simulations of oblique flow, the inlet volume is sloping. The inlet/outlet volumes are structurally meshed to reduce computational costs. Slip-wall boundary conditions are applied to inlet walls. For simulations with inlet flow perpendicular to the fabric, both slip-wall and periodic-wall boundary conditions were used; the difference in computed quantities between these boundary conditions was less than 2%. Velocity inlet and pressure outlet boundary conditions were chosen to define the inlet and outlet boundaries. **Figure 2** shows a representative cross section of the hybrid

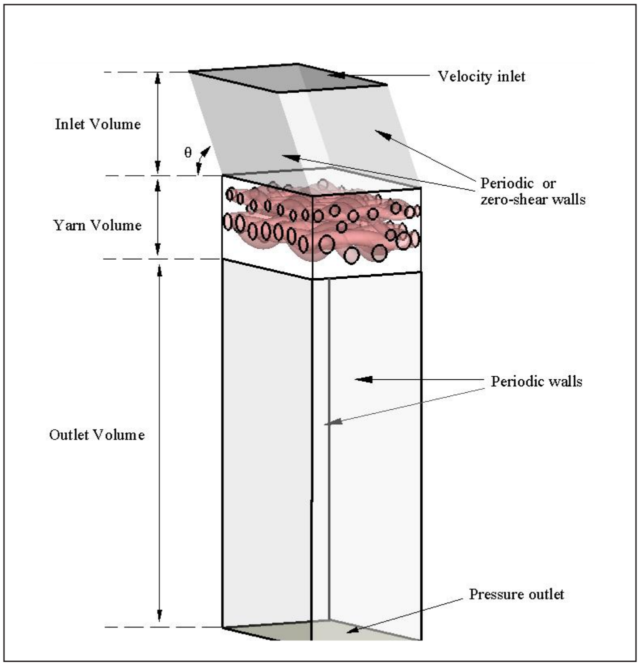

3. Computational geometry indicating the inlet, yarn, and outlet volumes.

mesh used for simulations. **Figure 3** shows a typical computational domain for inclined simulations. **Table I** gives the general specification of Fabric A used in simulations. Mesh is the number of yarns in the machine direction (MD) in 1 in. or 1 cm and knock is the number of yarns in the cross direction (CD) in 1 in. or 1 cm.

The meshed geometry was then imported into the computational fluid dynamic (CFD) package Fluent™ (ANSYS Inc., Canonsburg, PA) to create a CFD simulation of the flow-through fabrics. The governing equations to be solved were the conservation of mass and momentum equations for a Newtonian fluid. Because of the low Reynolds numbers for the flow, generally less than 40 based on filament diameter and bulk velocity, the steady laminar viscous model was used to specify the flow. In cases where the Reynolds number was higher, we ran the simulations with an unsteady solver as well. The discrepancy between the results of the two solvers was less than 2%.

Mesh independence and discretization error

Any CFD simulation should be run with meshes of different density to ensure that the results are independent of the mesh. We have conducted simulations for one fabric geometry by gradually refining the mesh. For a given pressure drop of a 125 Pa across the fabric, the average velocity on a mesh with 2.5 million cells differed by less than 0.05% from the velocity computed with a mesh with 3.5 million cells. Therefore, most of the simulations reported here were run on a grid of approximately 2.5 million cells.

As the mesh size approaches zero, a CFD solution should produce a solution to the continuum partial differential equations. To quantitatively estimate the size of the discretization error, we followed the procedure proposed by Roache [22]. The maximum numerical uncertainty in the fine-grid solution for the velocity through the fabric was found to be 0.05%, consistent with 0.05% difference computed in the previous section.

Comparison with experiment

The forming fabric manufacturer provided us with experimental measurements of fabric flow for Fabric A and for Fabric B, which is similar to Fabric A, but slightly different in mesh size and weave pattern. Air at a gauge pressure of 125 Pa on one side of a forming fabric was supplied and the flow rate (in ft^3/ min) through a 7 cm (2.75 in.) diam portion of the fabric was measured. In our companion article [1], we showed that the air permeability of the simulations is within 1% of those experimental results. **Table II** shows the comparison. The good agreement between simulation and experiments validates the CFD code and the way fabrics are modeled.

RESULTS AND DISCUSSION

Single layer vs. multilayer fabrics

It is worthwhile to analyze in detail the effects that a machine-side layer produces on the flow characteristics of a single-layer fabric. To achieve this, the computer-aided design model of Fabric A was cut on a plane between the layers, and CFD simulations were run for each layer separately. A comparison

Mesh/knock (1/in.) Mesh/knock (1/cm)			Air permeability (ft^3 /min) (m/s)	Yarn size (mm)			
Total	Paper side	Machine side		Paper side		Machine side	
146 x 186 58 x 74	73 x 93 29 x 37	73 x 62 29 x 24	440 2.2	0.13	0.13	0.21	0.20

I. General specification of Fabric A used in simulations.

	Simulations (ft^3 /min)	Experiments (ft^3 /min)	Difference %
Fabric A	436	440	0.9
Fabric B	354	352	0.6

II. Air permeability comparison between simulations and experimental data. The applied pressure drop across the fabric is 125 Pa.

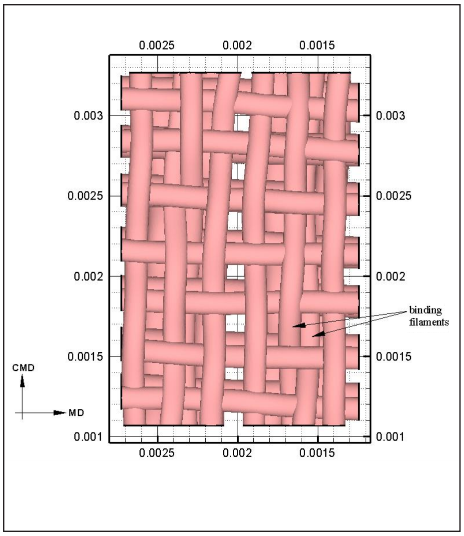

4. Top view of Fabric A; X and Y axes are in meters.

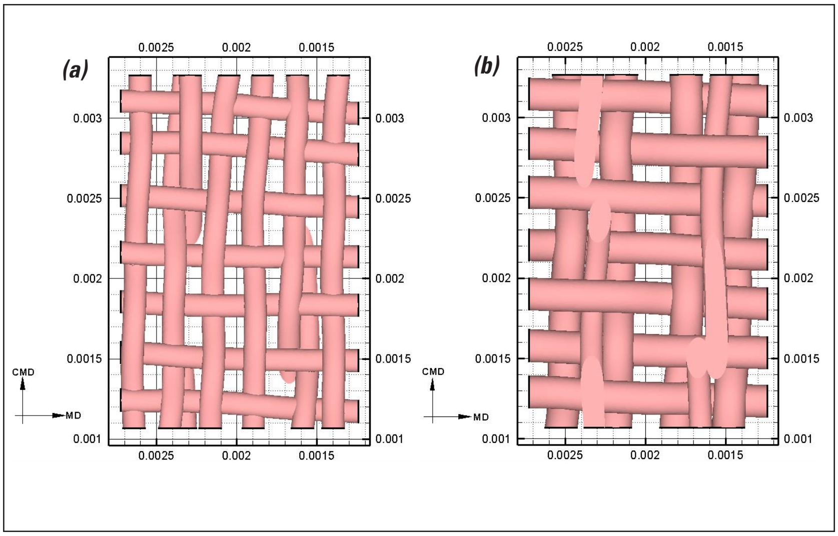

5. Top view of layers composing Fabric A: (a) paper-side layer, (b) machine-side layer. X and Y axes are in meters.

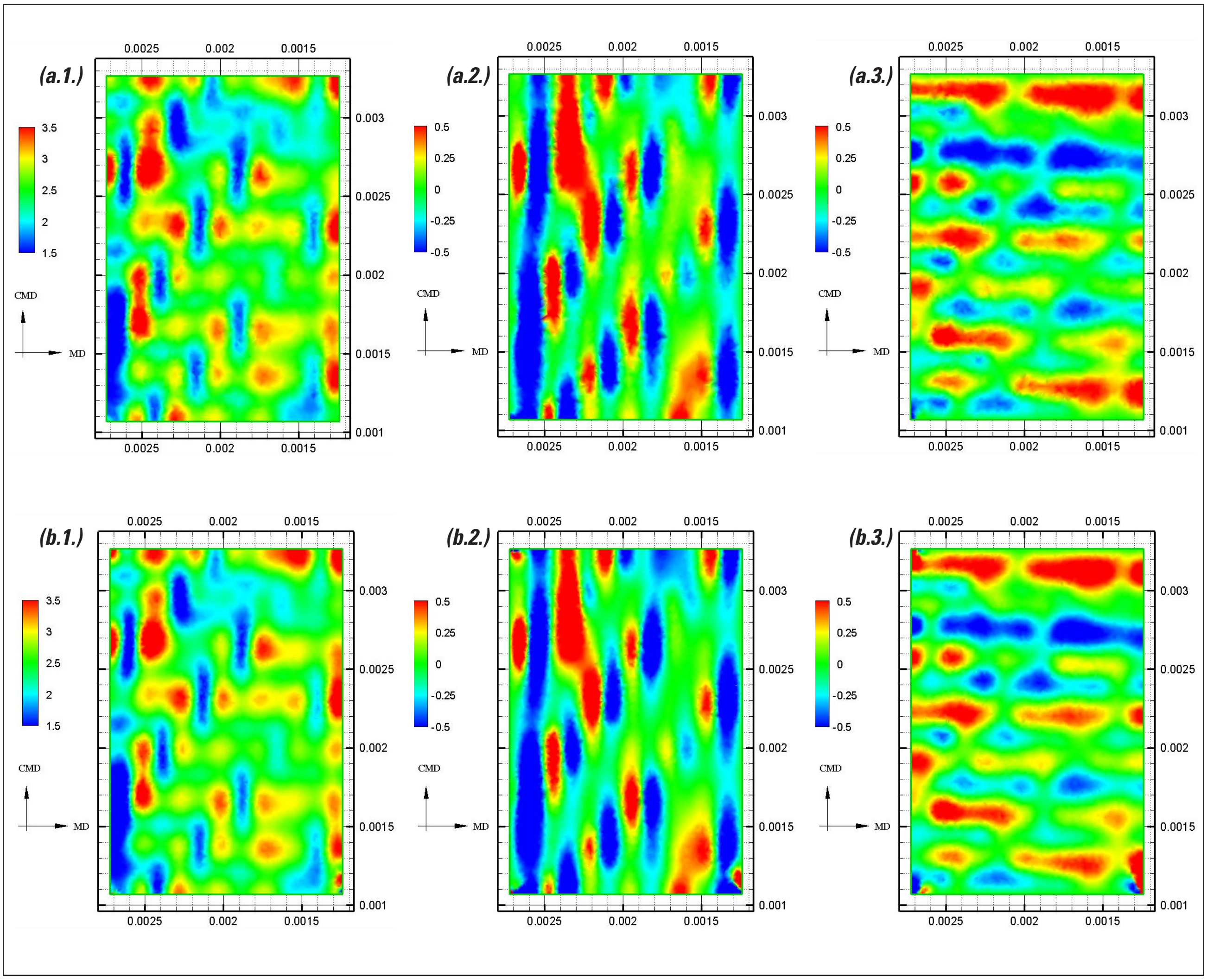

6. Point wise velocity contours of Z-direction, machine-direction, and cross-direction velocities. Velocities are in m/s: (a) full Fabric A, (b) paper-side layer of Fabric A.

between the flow fields are given in the following sections. **Figure 4** depicts the top view of Fabric A. **Figure 5** shows the constituent layers of the fabric. The binding filaments may be regarded as a center layer between the paper side and machine side of the fabric [23], but here we considered them as part of both the top and bottom layers.

Velocity contours

Figure 6 shows the Z-direction, machine-direction, and cross-directions components of fluid velocity through the complete Fabric A, as well as the same velocity components for its paper-side layer computed in isolation. The contours were extracted on a plane d/4 upstream away from the highest point of the paper-side layer (d = paper-side filament diameter). There was surprisingly little difference between the corresponding velocity contours, which implies that the paper-side layer plays a dominant role on the flow in the pulp suspension.

Averaged velocity contours

Typical pulp fibers are 0.3–3 mm long and should respond to some average velocity over their length rather than a local velocity. We followed the procedure described in our earlier work [1] to perform this velocity averaging. We performed elliptical averaging over an area comparable to the cross-sectional area of a fiber for both the full Fabric A and its paper-side layer only, and then subtracted the resulting contours. The results of such averaging for an ellipse with semimajor axis of 0.2 mm and semiminor axes of 0.02 mm, are shown in **Fig. 7** (ellipse major axis in MD) and **Fig. 8** (ellipse aligned with CD). The difference between paper-side-only and full-fabric velocities is up to approximately ± 15% of the mean velocity.

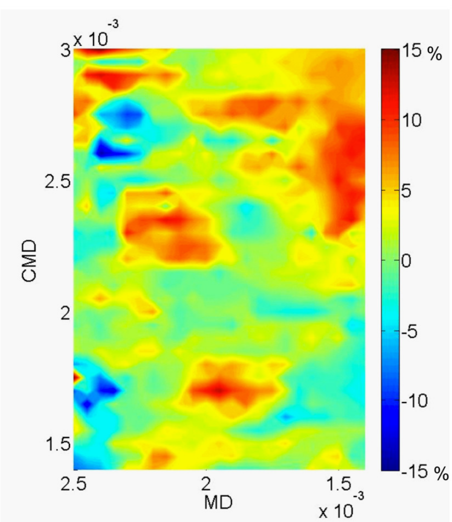

7. Spatial variation of difference between Z-direction velocities when averaged over an ellipse with semimajor axis = 0.2 mm and semiminor axis = 0.02 mm. The difference is normalized by the mean velocity. The ellipse is aligned with MD.

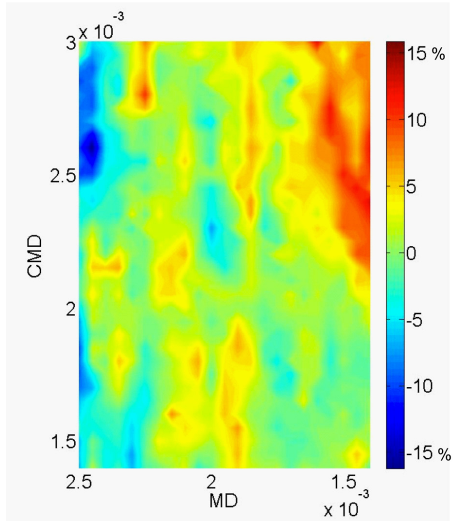

8. Spatial variation of difference between Z-direction velocities when averaged over an ellipse with semi-major axis = 0.2mm and semi-minor axis = 0.02mm. The difference is normalized by the mean velocity. The ellipse is aligned with CD.

Pressure drop versus flow rate

Simulations were run for a number of different inlet velocities for Fabric A and its layers separately. The dimensionless pressure drop was thus determined as a function of the Reynolds number. Here, Re = VD/ν where V is the bulk velocity of the fluid through the fabric, D is the filament diameter for filaments on the paper side (= 0.125 mm), and ν is the kinematic viscosity of the fluid. The static pressure drop, Δp, is made dimensionless in the form of a pressure drop coefficient given by $C_P = \Delta p / 0.5 \rho V^2$, where ρ is the fluid density. The C_P - Re curves are well described by a power law, with high coefficient of determination, as shown in **Figure 9**. Surprisingly, the power on the Reynolds number for all curve fits is about -0.36. Interestingly, the exponent on the Reynolds number is almost half way between the creeping flow limit ($C_P \propto \mathrm{Re}^{-1}$) and the

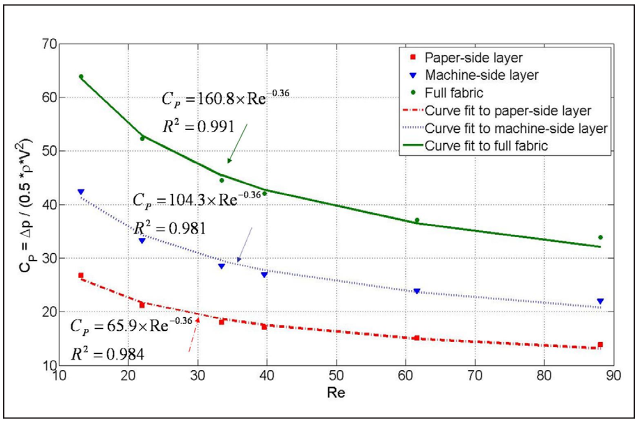

9. C_p – Re curve for full Fabric A and its layers.

Re	14	22	33	40	62	88
C_P, paper	27	21	18	17	15	14
C_P, machine	42	33	29	27	24	22
$\Sigma\ C_P$	69	54	47	44	39	36
C_P, both	64	52	44	42	37	34
% difference	7	2	2	2	5	3

III. Comparison of the pressure drop through a full fabric and its layers.

fully developed turbulence limit ($C_P \propto \mathrm{Re}^0$). As seen in **Table III**, the pressure drop through the entire forming fabric is nearly equal to the sum of the pressure drops through the two layers. In addition, because extra surface area is exposed when the binder filaments are cut through, it could be anticipated that the sum of the two half-fabric resistances would slightly exceed that of the full fabric. This effect alone may account for the majority of the (already small) differences seen in Table III.

Oblique versus perpendicular dewatering

In all previous simulations, the approach flow was taken normal to the fabrics, i.e., we neglected the speed ratio between the jet and the fabric. In this section we consider approach flows $58° \leq \theta \leq 90°$, corresponding to impingement angles $3° \leq \alpha \leq 15°$ and $0.99 \leq R_{JW} \leq 1.035$. Slip walls are assumed for the inlet walls rather than periodic walls, as were used in previous simulations. Moreover, simulations were run on a Fabric C, which has the same weave pattern as Fabric A, but with somewhat thinner strands.

We ran simulations for different inlet velocities while changing the impingement angle. The calculated pressure drops across the fabric were converted into pressure coefficients. The pressure coefficient versus Reynolds number curve varied only slightly as the impingement angle was changed from 58° to 90° impingement. In other words, the fabric permeability varied only slightly between rush and drag conditions.

The most marked characteristic of rush or drag is expected to be observed in the shear stresses. To illustrate this, we averaged the machine-direction shear stress over elliptical areas aligned with the MD. The results of averaging were then normalized with the dynamic pressure and calculated based on the approach flow.

Figure 10 shows the contours of the elliptically averaged, normalized shear stress for different approach flow angles. There is an apparent similarity between the contours, but the mean value of the normalized shear stress for the 58° case was 0.011, whereas for 90° impingement it was -0.0013. As expected, the shear stress increased as the incoming flow became more parallel to the fabric. For flow perpendicular to an isotropic medium, zero mean shear stress would be expected. As seen in Fig. 5, the piece of fabric chosen for the flow analysis is far from isotropic, which explains why the mean shear stress for 90° impingement is not zero.

CONCLUSION

We ran simulations of flow-through 3D models of forming fabrics, built based on the procedure described in our earlier work [1]. The CFD simulations of the models were shown to predict the fabric permeability within 1% of experimental measurements. A specific fabric, Fabric A (and a variant thereof), was used to study two quantities on the flow-through of real forming fabrics: (1) the influence of machine-side filaments and (2) jet-to-wire speed ratio.

We found that the machine-side filaments had a small influence on the flow field upstream of the paper-side filaments and consequently on the initial fiber mass distribution of pulp

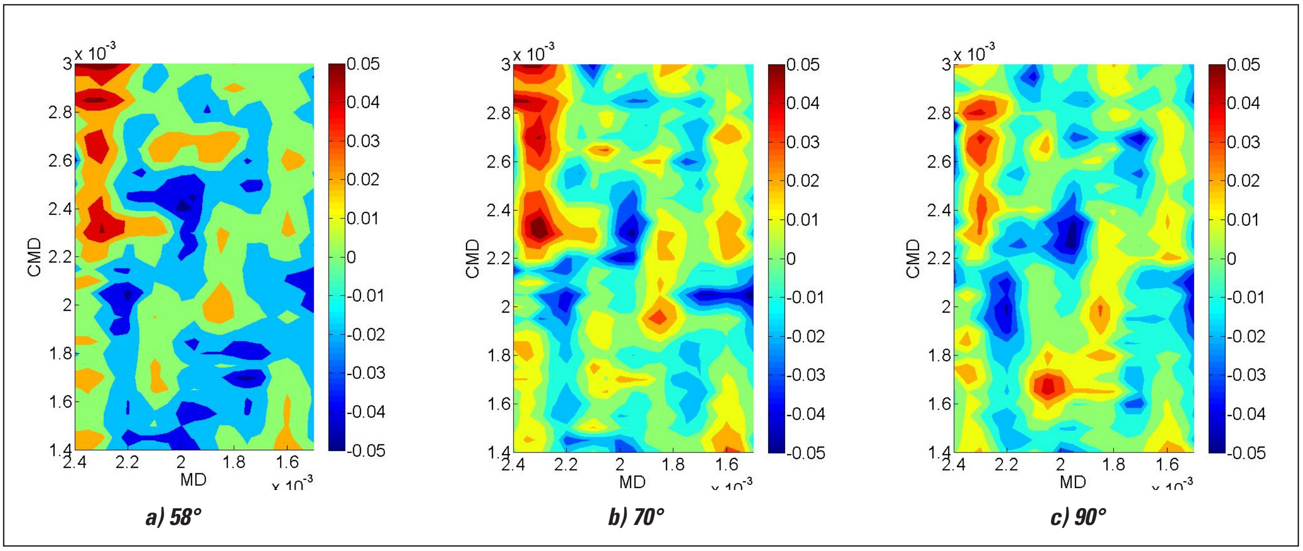

10. Spatial variation of nondimensional shear stress when averaged over an ellipse with semi-major axis = 0.2 mm and semiminor axis = 0.02 mm. The ellipse is aligned with MD. Owing to the unphysical imposed zero shear stress wall condition applied to MD 2.5 mm and MD = 1.4 mm, only the region of the fabric away from these walls is shown.

fibers. The pressure drop of a fabric was found to be approximately the sum of that through the paper-side and machine-side layers. Therefore, we concluded that the machine-side layer plays only a minor role on the upstream flow although it does increase the overall resistance of the fabric to the flow.

When we simulated the rush or drag of the impingement jet by inclining the inlet volume, the air permeability varied only slightly from 58° to 90° impingement. Rush or drag had a more pronounced effect on the MD shear stress, which will tend to orient fibers in the machine direction.

Flow simulations appear to be a powerful tool to characterize fabric resistance to flow and to predict the microscale nonuniform flow through multilayer forming fabrics. We aim to extend this work to calculate the probable fiber/fine mass distribution in a sheet, at the very early stage of water removal from pulp suspensions. **TJ**

ACKNOWLEDGMENTS

The authors appreciate the financial support of NSERC and AstenJohnson Inc.

LITERATURE CITED

1. Vakil, A., Olyaei, A., and Green S. I., *Nord. Pulp Paper Res. J.* 24(3): 338(2009)
2. Adanur, S., *Paper Machine Clothing*, Technomic Publishing, Lancaster, PA, USA, 1997.
3. Johnson, D.B., *Pulp Paper Can.* 85(6): 126(1984).
4. Johnson, D.B., *Pulp Paper Can.* 87(5): 56(1986).
5. Danby, R., *Pulp Paper Can.* 87(6): 69(1986).
6. Helle, T., *J. Pulp Paper Sci.* 14(4): J91(1988).
7. Antoine, C., *Appita J.* 60(3): 196(2007).
8. Danby, R., *Pulp Paper Can.* 95(1): 48(1994).
9. Danby, R., *Pulp Paper Can.* 101(9): 66(2000).
10. Helle, T., *Pulp Paper Can.* 21(4): 123(1980).
11. Adanur, S., *Tappi J.* 77(10): 187(1994).
12. Helle, T., Pulp Paper Can. 79(11): 91(1978).
13. Ingmanson, W.L., Han, S.T., Wilder, H.D., et al., *Tappi* 44(1): 54(1961).
14. Armour, J.C. and Cannon, J.N., *Am. Inst. Chem. Eng.* 14(3): 415(1968).
15. Rushton, A. and Griffiths, P., *Transactions of the Institution of Chemical Engineers* 49: 49(1971).
16. Pedersen, G.C., *Filtration and Separation* 11(12): 586(1974).
17. Chhabra, R.P. and Richardson, J.F., *Chem. Eng. Sci.* 40(2): 313(1985).
18. Huang, Z., "Numerical simulations of flow through model paper machine forming fabrics," Master's thesis, The University of British Columbia, Vancouver, BC, 2003.
19. Gilchrist, S., :Experimental investigation of a model forming fabric," Master's thesis, The University of British Columbia, Vancouver, BC, 2006.
20. Green, S. I, Wang, Z., Waung, T., et al., *Comput. and Fluids* 37(9): 1148(2008).
21. Guesalaga A. R., Cabezas F.M., and Gottschalk C., *Meas. Sci. Technol.* 8: 574(1997).
22. Roache, P.J., *Ann. Rev. Fluid. Mech.* 29: 123(1997).
23. Xu, J., Danby, R., Johnson, D., and VandeKolk, J., *Proceedings, 95th EXFOR and Annual Meeting*, PAPTAC, Montreal, QC, Canada, 2009, p. 343.

ABOUT THE AUTHORS

Our goal was to answer some longtime questions from papermakers on the influence of machine-side filaments on the flow characteristics of forming fabrics. Previously, we studied the resistance of multilayer fabrics to the flow. In this research, we extended the work to investigate the effect of each forming fabric layer as well as the effect of the angle of the approach flow.

Our biggest challenge was to conduct complete, 3D, and mesh-independent CFD simulations of the flow through forming fabrics. We described a novel method to model fabrics and produced computational domains to simulate the flow. The most surprising finding was the dependence of the pressure drop on the Reynolds number of the flow at these moderate Reynolds numbers, and the serial resistance of layers to the flow.

Information from this study can give fabric suppliers to mills some insight into the tradeoff between selecting fabrics for long life and superior drainage/retention characteristics. Whereas this research paper simulated the rush and drag of jet impingement by tilting the inlet volume of the simulations, a more comprehensive study might take into account the free surface interaction of the pulp suspension and the surrounding air.


Vakil


Olyaei


Green

Vakil is graduate research assistant, Olyaei is research assistant, and Green is professor and head of the Department of Mechanical Engineering, University of British Columbia Pulp and Paper Centre, Vancouver, BC. Email Green at green@mech.ubc.ca.